Supporting Information

Effect of Silica Surface Properties on the Formation of Multilayer or Submonolayer Protein Hard Corona: Albumin Adsorption on Pyrolytic and Colloidal SiO_2 Nanoparticles

Federico Catalano,[#] Gabriele Alberto,[†,] Pavlo Ivanchenko,[†] Galyna Dovbeshko[‡] and Gianmario Martra[†,]**

#Department of Clinical and Biological Sciences, University of Torino, Regione Gonzole 10, 10043 Orbassano (TO), Italy

†Department of Chemistry and Interdepartmental Nanostructured Interfaces and Surfaces (NIS) Centre, University of Torino, via P. Giuria 7, 10125 Torino, Italy;

‡Institute of Physics of the National Academy of Science of Ukraine, 46 Nauki Ave., Kyiv 03028, Ukraine.

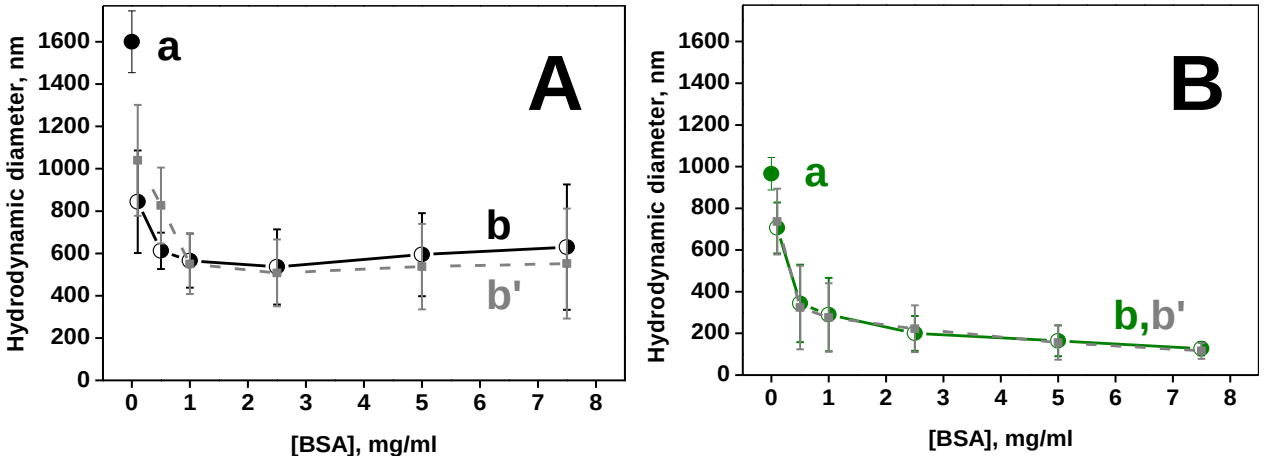

Figure S1. Hydrodynamic diameters resulting from the mean values of mass distributions obtained in DLS measurements for P-SiO_2 and M-SiO_2 (panel A and B, respectively) suspended in: a) PBS (single points); b) PBS, after incubation with BSA at different concentrations (0.1-7.5 mg·mL^{-1}) and removal of not adsorbed and reversibly adsorbed BSA (solid line curves); b') in PBS after incubation and in equilibrium with proteins (dashed line curves).

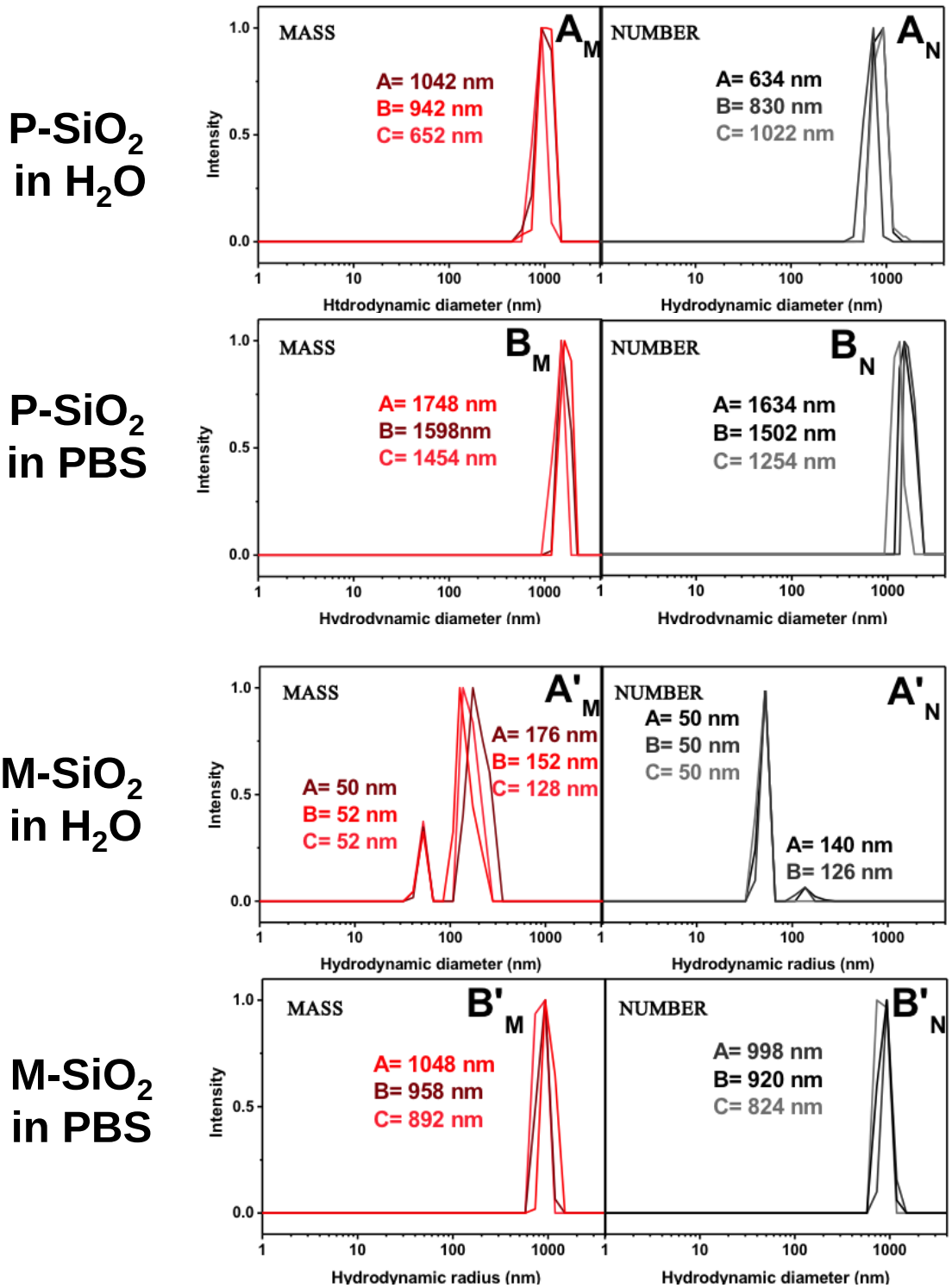

Figure S1, *continued.* Raw data of DLS measurements related to values presented in the main text. All the data are presented both in mass (left panels, labeled as "X_M") and number (right panels, labeled as "X_N") distributions. Each measure of the triplicates is reported: P-SiO_2 and M-SiO_2 in MilliQ water (A and A', respectively), P-SiO_2 and M-SiO_2 suspended in PBS (B and B', respectively).

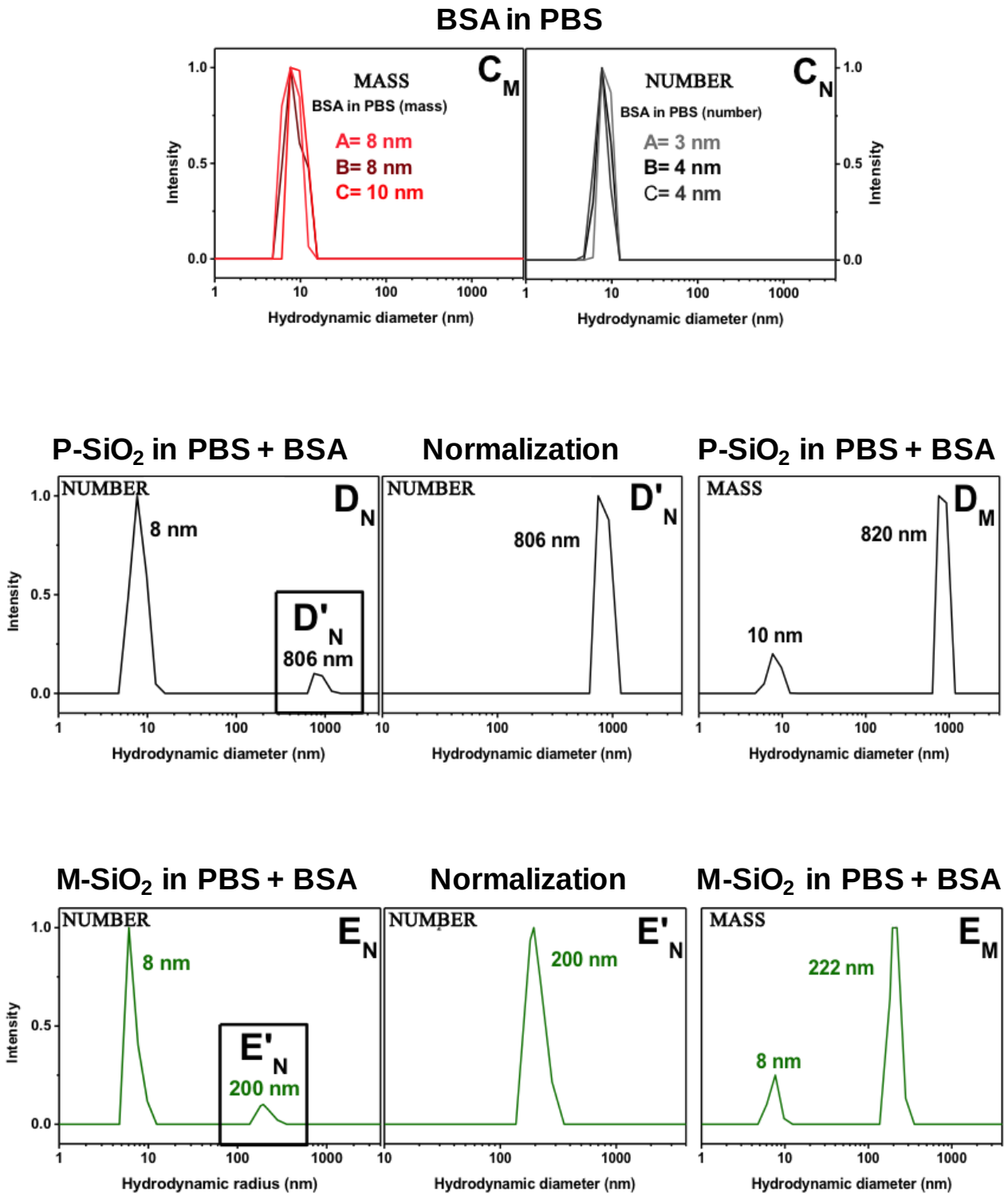

Figure S1, ***continued***. Raw data of DLS measurements of BSA in PBS (C) and of NPs in PBS in equilibrium with BSA (D,E). Given the prevalence, in the number distributions, of the signal related to the presence of proteins in solution (HD = ca. 8 nm), significantly more intense then the signal due to NP agglomerates, number distributions of hydrodynamic diameters of NPs were normalized as reported in panels D' and E' for P-SiO_2 and M-SiO_2, respectively.

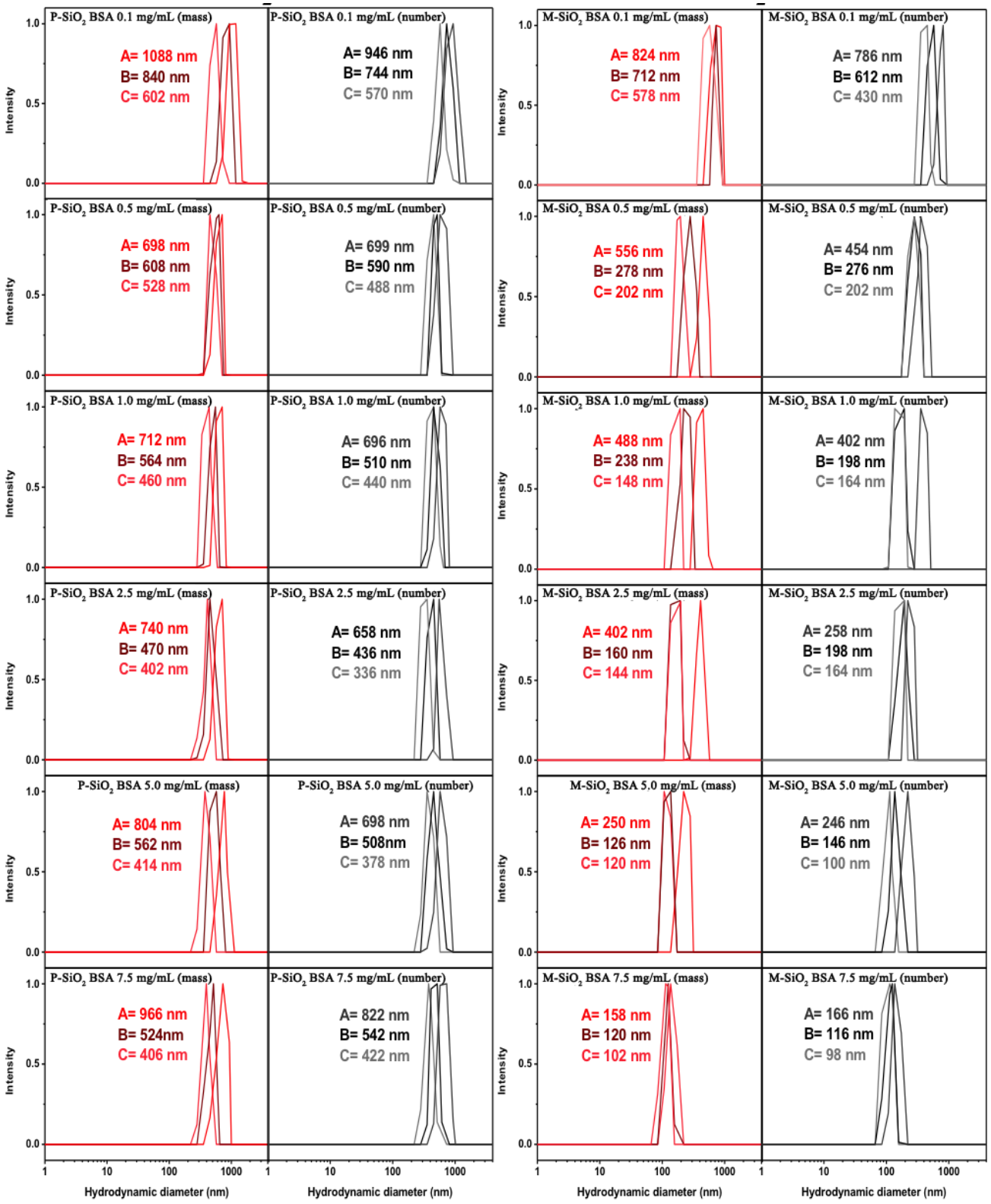

Figure S1, ***continued***. Raw data of DLS measurements of P-SiO_2 and M-SiO_2 (F and G, respectively) resuspended in bare PBS after incubation with BSA (0.1-7.5 $mg \cdot mL^{-1}$) and removal of not adsorbed and reversibly adsorbed BSA through centrifugation/resuspension cycles.

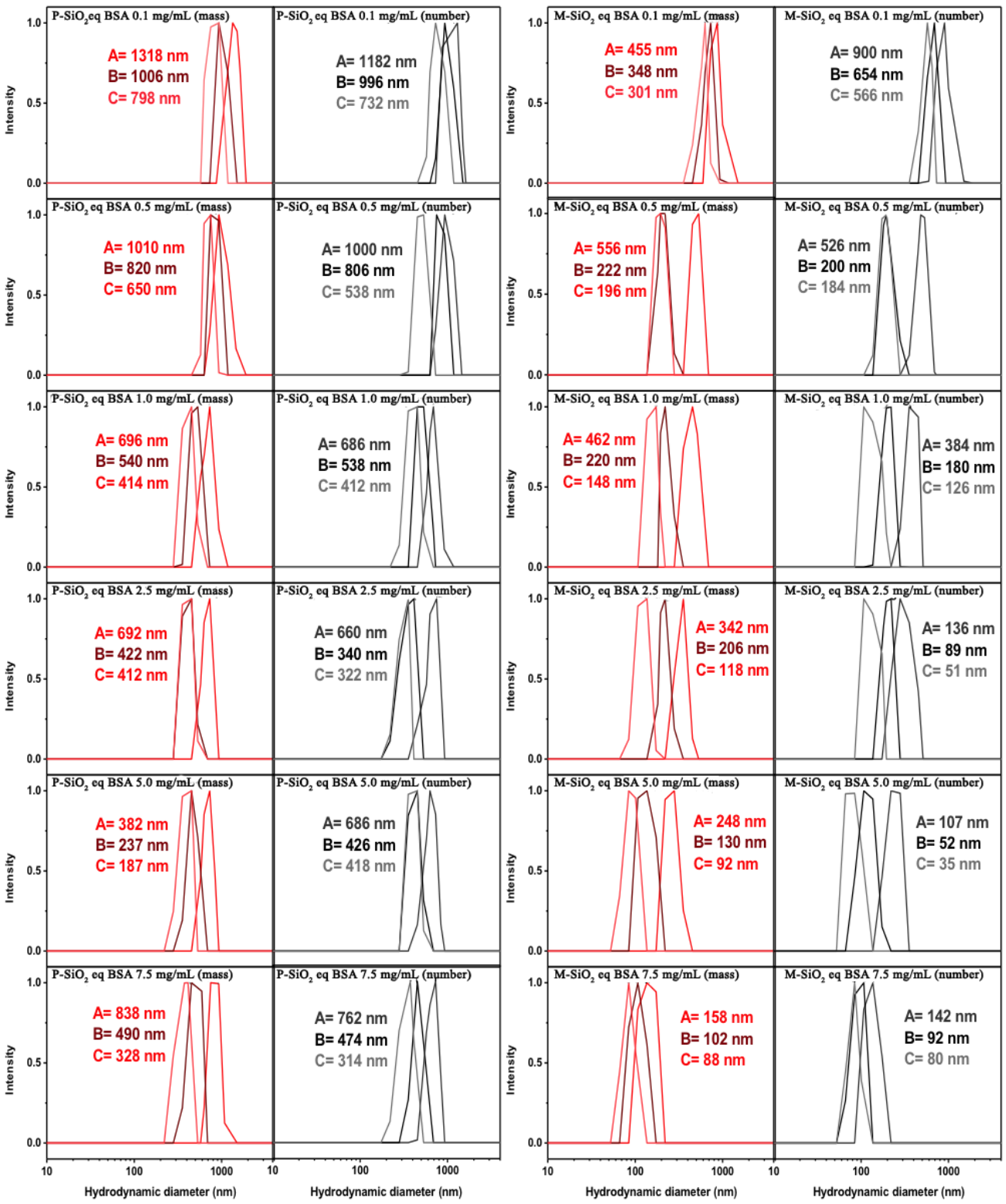

Figure S1, ***continued***. Raw data of DLS measurements of P- and M-SiO_2 (H and I respectively) suspended in PBS after incubation and in equilibrium with BSA at different concentration (0.1-7.5 $mg \cdot mL^{-1}$); data are normalized as reported in panel (D',E') and the contribution of BSA omitted.

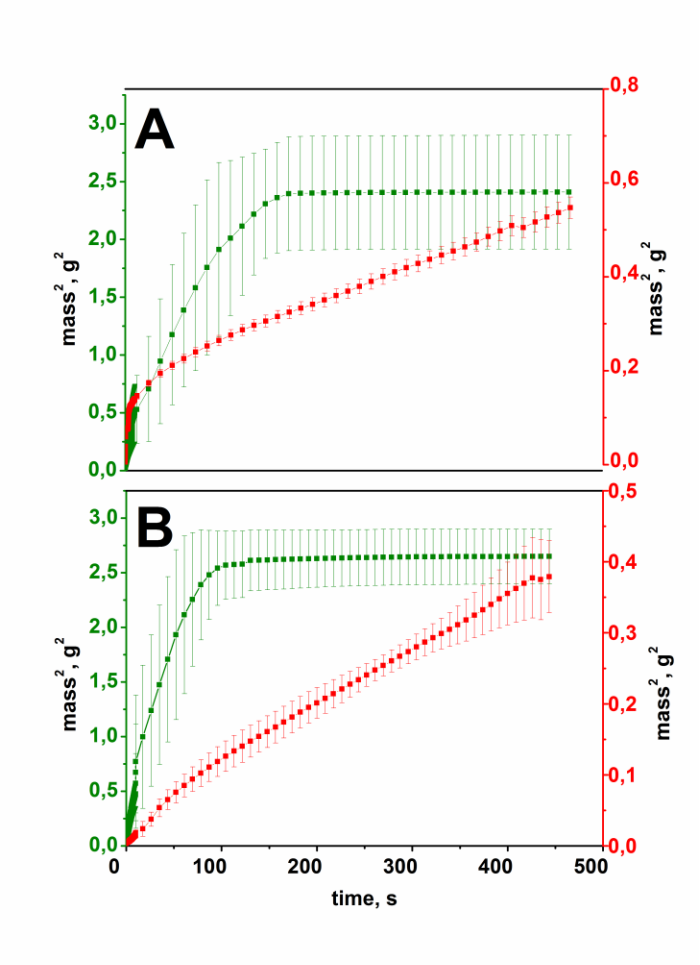

Figure S2. Kinetics of capillary rise of MilliQ water (A) and PBS solution (B) in P-SiO_2 (red curves) and M-SiO_2 (green curves) packed samples.

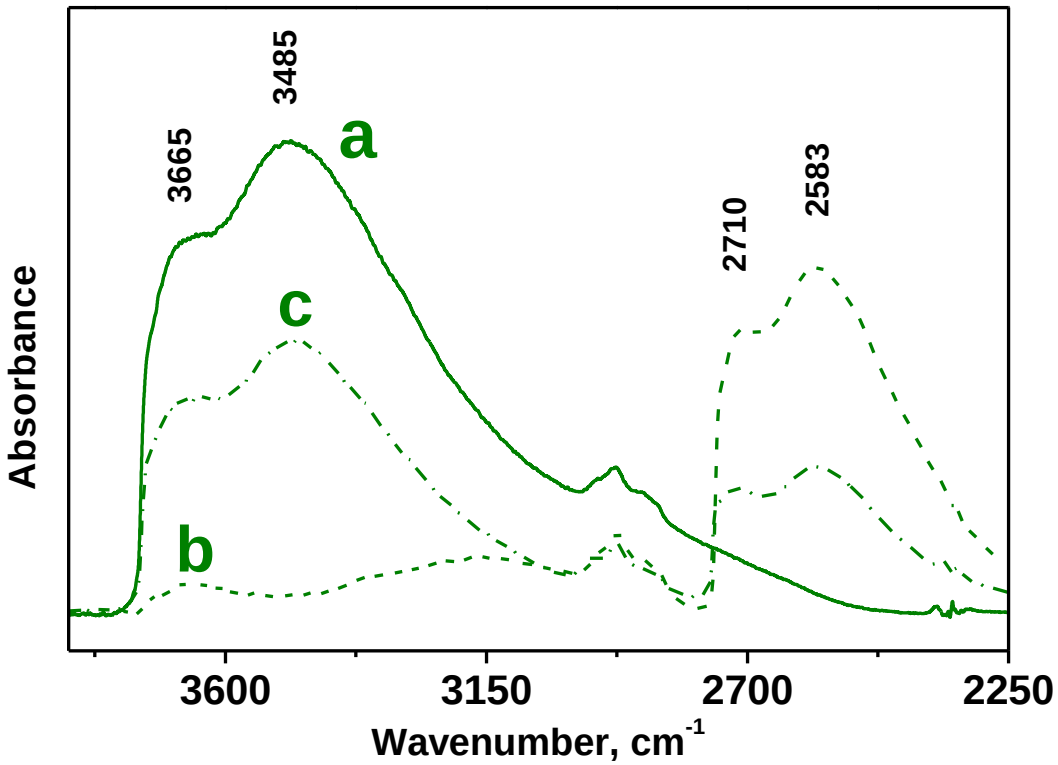

Figure S3. IR spectra, in the 3800-2250 cm^{-1} range, of M-SiO_2: a) outgassed at b.t.; b) after H/D exchange by contact with D_2O and subsequent outgassing at b.t. cycles until invariability of spectra; c) after back D/H exchange by contact with tert-butanol cycles, until invariability of spectra. On the basis of the integrated area of the νOH and νOD pattern, the silanols sensitive to the D/H back exchange resulted to be ca. 60% of the total.

Table S1. Data set used for the calculation of the layers of adsorbed BSA with respect a theoretical side-on monolayer (θ=1), corresponding to 2250 μg of BSA per·m^{-2}.[1] Nanoparticle agglomerates where assumed to be spherical for the calculation of their volume and surface area, with diameters corresponding to the values obtained by DLS (see Figure 4A in the main text). For the calculation of the mass of NPs agglomerates a specific mass of 2.2 g·cm^{-3}, previously measured for M–SiO_2, and similar to what expected for amorphous silica, was used.[2]

sample + BSA (mg·mL^{-1})	Diameter of NPs agglomerates (nm)	Volume of 1 NPs agglomerate (nm^3)	Mass of 1 NPs agglomerate (mg)	Number of NPs agglomerates in 50 mg of NPs	Surface area of 1 NPs agglomerates (nm^2)	Total surface area of NPs agglomerates in 50 mg of NPs (m^2)	Mass of BSA adsorbed on 50 mg of NPs (μg)	Mass of BSA adsorbed per surface unit of NPs agglomerates (μg·m^{-2})	BSA layers with respect a theoretical side-on monolayer (Θ=1)
P-SiO₂ (PS)	1600	$2.14\cdot10^{9}$	$4.71\cdot10^{-9}$	$1.06\cdot10^{10}$	$8.04\cdot10^{6}$	0.09	0	0	0
PS+BSA 0.1	844	$3.14\cdot10^{8}$	$6.92\cdot10^{-10}$	$7.22\cdot10^{10}$	$2.24\cdot10^{6}$	0.17	121	749	0.3
PS+BSA 0.5	612	$1.20\cdot10^{8}$	$2.63\cdot10^{-10}$	$1{,}89\cdot10^{11}$	$1.17\cdot10^{6}$	0.24	493	2215	1.0
PS+BSA 1	566	$9.48\cdot10^{7}$	$2.09\cdot10^{-10}$	$2.39\cdot10^{11}$	$101\cdot10^{6}$	0.26	871	3613	1.6
PS+BSA 2.5	536	$8.06\cdot10^{7}$	$1.77\cdot10^{-10}$	$2.82\cdot10^{11}$	$9.02\cdot10^{5}$	0.28	1161	4562	2.0
PS+BSA 5	594	$1.09\cdot10^{8}$	$2.41\cdot10^{-10}$	$2{,}07\cdot10^{11}$	$1.11\cdot10^{6}$	0.25	1208	5262	2.3
PS+BSA 7.5	630	$1.03\cdot10^{8}$	$2.88\cdot10^{-10}$	$1.74\cdot10^{11}$	$1.25\cdot10^{6}$	0.23	1493	6895	3.1
M-SiO₂ (MS)	966	$3.49\cdot10^{8}$	$7.68\cdot10^{-10}$	$6.51\cdot10^{10}$	$2.93\cdot10^{6}$	0.15	0	0	0
MS+BSA 0.1	706	$1.36\cdot10^{8}$	$3.00\cdot10^{-10}$	$1.67\cdot10^{11}$	$1.56\cdot10^{6}$	0.21	72	276	0.1
MS+BSA 0.5	344	$1.58\cdot10^{7}$	$3.47\cdot10^{-11}$	$1.44\cdot10^{12}$	$3.71\cdot10^{5}$	0.46	274	512	0.2
MS+BSA 1	290	$9.45\cdot10^{6}$	$2.08\cdot10^{-11}$	$2.41\cdot10^{12}$	$2.64\cdot10^{5}$	0.57	362	569	0.3
MS+BSA 2.5	200	$3.10\cdot10^{6}$	$6.82\cdot10^{-12}$	$7.34\cdot10^{12}$	$1.26\cdot10^{5}$	0.91	1225	1330	0.6
MS+BSA 5	164	$1.71\cdot10^{6}$	$3.76\cdot10^{-12}$	$1.33\cdot10^{13}$	$8.44\cdot10^{4}$	1.20	1020	907	0.4
MS+BSA 7.5	126	$7.75\cdot10^{5}$	$1.70\cdot10^{-12}$	$2.93\cdot10^{13}$	$4.99\cdot10^{4}$	1.79	1664	1138	0.5

[1] Rezwan, K.; Meier, L.P.; Rezwan, M.; Vörös, J.; Textor, M.; Gauckler, L.J., *Langmuir* **2004**, 20, 10055-10061
[2] Alberto G., Miletto I.,. Viscardi G, Caputo G., Latterini L., Coluccia S., Martra G., *J. Phys. Chem. C* **2009**, 113, 21048-21053

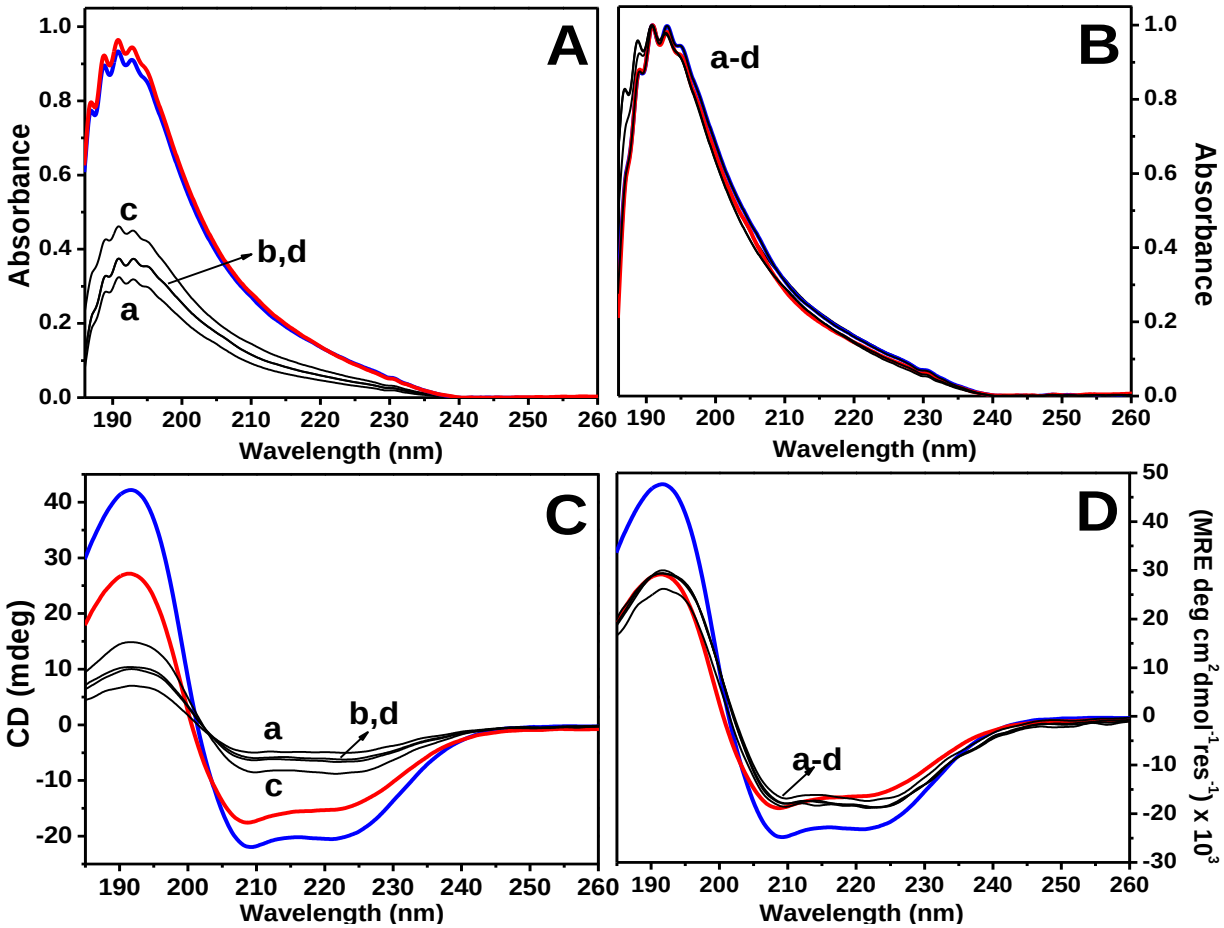

Figure S4. Absorbance (panels A, B) and CD-UV (panels C, D) spectra of: BSA in solution and after thermal treatment (blue and red lines, respectively), and BSA irreversibly adsorbed on silica NPs after incubation in PBS (protein concentrations; 0.5, 2.5, 5.0 and 7.5 mg·mL^{-1}, curves a, b, c and d, respectively) and subsequent centrifugation/washing cycles. After the last centrifugation nanoparticles with irreversibly adsorbed proteins were resuspended in MilliQ water, to attain a proper transparency in the spectral range investigated.

Comment to the figure:
Suspensions of agglomerates of silica M-SiO_2 and P-SiO_2 carrying the irreversible fraction of adsorbed proteins were prepared by controlling the amount of sample in order to attain the same nominal concentration of proteins in unit volume of the samples. The amount of adsorbed proteins per mass of silica agglomerate obtained by UV measurements and the mass of silica used for the incubation with BSA solutions were used as data base. Despite the nominal equivalency of the amount of BSA present in such samples, significant differences were obtained in the intensity of the absorption signals in the 180-260 nm range due to $\pi \rightarrow \pi^*$ and $n \rightarrow \pi^*$ transitions of the carbonylic groups in the polypeptide backbone (panel A). The origin of such discrepancy was the inhomogeneity and instability of the suspension of the samples during the measurements. Thus, the Absorbances were normalized to a common intensity value (panel B), and the normalization factors were used for the normalization of the corresponding CD-UV spectra (panel C: original; panel D: normalized). It is worth to notice that such data elaboration did not affect the shape of the CD-UV lines, and then the information contained in the change of the relative intensity of the negative bands at 208 and 222 nm with respect BSA in solution.